Journal of Sound and Vibration (1997) **203**(3), 435–446

DETECTION OF THE LOCATION AND SIZE OF A CRACK IN STEPPED CANTILEVER BEAMS BASED ON MEASUREMENTS OF NATURAL FREQUENCIES

B. P. NANDWANA AND S. K. MAITI

Department of Mechanical Engineering, Indian Institute of Technology, Bombay, Mumbai—400 076, *India*

(*Received* 12 *September* 1995, *and in final form* 6 *November* 1996)

A method based on measurement of natural frequencies is presented for detection of the location and size of a crack in a stepped cantilever beam. The crack is represented as a rotational spring, and the method involves obtaining plots of its stiffness with crack location for any three natural modes through the characteristic equation. The point of intersection of the three curves gives the crack location. The crack size is then computed using the standard relation between stiffness and crack size. An example to demonstrate the usefulness and accuracy of the method is presented.

1. INTRODUCTION

Vibration based methods of detection of a crack offer some advantages. They can help to determine the location and size of a crack from the vibration data collected from a single point on the component. When a crack develops in a component, it leads to a reduction in the stiffness and an increase in its damping [1]. This, in turn, gives rise to a reduction of natural frequencies and a change in the mode shapes. These effects are mode dependent. Hence, it may be possible to estimate the location and size of a crack by measuring changes in the vibration parameters. These could include either the modal parameters or the structural parameters. The modal parameters include natural frequencies and mode shapes, and the structural parameters are the stiffness, mass, flexibility and damping matrices of the system. A vibration based method of crack detection utilizes any one of the above as the key parameter.

In all of the methods, the modelling of damage is important. Petroski [2] has proposed a technique in which the section modulus is appropriately reduced to model a crack. Grabowski [3], Mayes and Davies [4] and Christides and Barr [5] have employed the same technique to study cracked rotors. Another approach has been to model the crack by a local flexibility matrix [6], the dimensions of which depend on the degrees of freedom being considered. Several researchers have determined various elements of this matrix, and a complete 5×5 matrix (neglecting torsion) has been presented in reference [6]. In the case of transverse vibrations, the dimension of the flexibility matrix is reduced. Dimarogonas and Papadopoulos [7] have computed a flexibility matrix for a transverse surface crack on a shaft. Papadopoulos and Dimarogonas [8] have modelled the coupled longitudinal and bending vibrations of a cracked shaft by a 2×2 flexibility matrix. In the case of transverse vibrations of beams this concept reduces to one of representing the crack by a rotational spring inserted at the site of the crack [9–12]. The stiffness of the spring depends upon the size of the crack. Ostachowicz and Krawczuk [12] have obtained equivalent stiffness of open double-sided and single-sided cracks, and have studied the effects of two open cracks upon the natural frequencies of flexural vibrations of a cantilever beam.

Adams *et al*. [13] have presented a method for detection of damage in a one-dimensional component utilizing the natural frequencies of longitudinal vibrations. They modelled the

0022–460X/97/230435 + 12 $25.00/0/sv960856

damage by a linear spring and employed the receptance method for analysis. Cawley and Adams [14] have given a method suitable for two-dimensional components using sensitivity analysis and finite element modelling of the damage. Chondros and Dimarogonas [9] have used the concept of a rotational spring to model the crack and given a method to identify cracks in welded joints. Rizos *et al*. [10] have applied this technique and detected the crack location through the measurement of amplitudes at two points on the component. Liang *et al*. [11] have studied a similar problem and have also represented the crack by a massless rotational spring. The latter investigators indicate that, for a given natural frequency and crack location, the characteristic equation can be solved to obtain the numerical value of the stiffness.

Kam and Lee [15] have given a method of crack detection using modal test data. Pandey *et al*. [16] have proposed the measurement of curvature mode shapes. Another method has also been proposed, based on changes in flexibility [17].

The method based on the rotational spring has always been applied to beams of uniform cross-section. There is a need to examine whether it can be applied to more realistic beam configurations, e.g. stepped beams. In this paper, the method [10, 11] is applied to a stepped cantilever beam (see Figure 1).

2. FORMULATION

The crack, located at a distance e from the fixed end, is represented by a rotational spring of stiffness K_t. The governing equation of flexural vibration is given by

$$\frac{d^2}{dx^2}\left(EI\frac{d^2U}{dx^2}\right) + \omega^2\rho AU = 0, \tag{1}$$

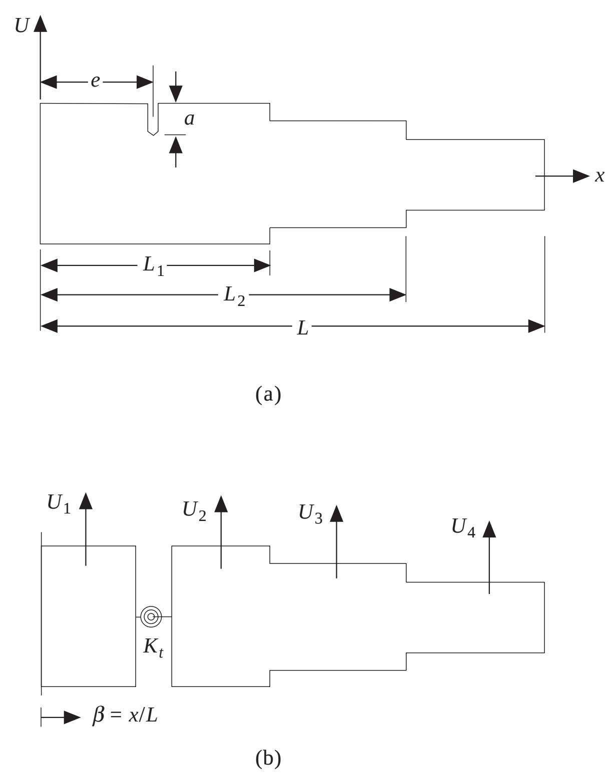

Figure 1. (a) The stepped cantilever beam. (b) The rotational spring representation of the crack.

where ω is the natural frequency. The four beam segments can be treated separately. The equations for the four segments are as follows:

$$\mathrm{d}^4 U_1/\mathrm{d}\beta^4 + \lambda_1^4 U_1 = 0, \qquad 0 \leqslant \beta \leqslant e/L, \tag{2}$$

$$\mathrm{d}^4 U_2/\mathrm{d}\beta^4 + \lambda_1^4 U_2 = 0, \qquad e/L \leqslant \beta \leqslant \beta_1, \qquad \beta_1 = L_1/L, \tag{3}$$

$$\mathrm{d}^4 U_3/\mathrm{d}\beta^4 + \lambda_2^4 U_3 = 0, \qquad \beta_1 \leqslant \beta \leqslant \beta_2, \qquad \beta_2 = L_2/L, \tag{4}$$

$$\mathrm{d}^4 U_4/\mathrm{d}\beta^4 + \lambda_3^4 U_4 = 0, \qquad \beta_2 \leqslant \beta \leqslant 1, \tag{5}$$

where $\lambda_1^4 = \omega^2 \rho A_1 L^4/EI_1$, $\lambda_2^4 = \omega^2 \rho A_2 L^4/EI_2$, $\lambda_3^4 = \omega^2 \rho A_3 L^4/EI_3$ and $\beta = x/L$. If there are more steps, the total number of equations will be equal to the number of steps plus one.

The solutions of the four segments can be written in the following form:

$$U_1 = A_1 \cosh \lambda_1 \beta + A_2 \sinh \lambda_1 \beta + A_3 \cos \lambda_1 \beta + A_4 \sin \lambda_1 \beta, \tag{6}$$

$$U_2 = A_5 \cosh \lambda_1 \beta + A_6 \sinh \lambda_1 \beta + A_7 \cos \lambda_1 \beta + A_8 \sin \lambda_1 \beta, \tag{7}$$

$$U_3 = A_9 \cosh \lambda_2 \beta + A_{10} \sinh \lambda_2 \beta + A_{11} \cos \lambda_2 \beta + A_{12} \sin \lambda_2 \beta, \tag{8}$$

$$U_4 = A_{13} \cosh \lambda_3 \beta + A_{14} \sinh \lambda_3 \beta + A_{15} \cos \lambda_3 \beta + A_{16} \sin \lambda_3 \beta, \tag{9}$$

where $A_1, \ldots, A_{16}$ are arbitrary constants. With every additional step, four more constants will appear.

The boundary conditions at the ends are as follows:

$$U_1 = 0, \qquad \mathrm{d}U_1/\mathrm{d}\beta = 0, \qquad \beta = 0, \tag{10}$$

$$\mathrm{d}^2 U_4/\mathrm{d}\beta^2 = 0, \qquad \mathrm{d}^3 U_4/\mathrm{d}\beta^3 = 0, \qquad \beta = 1. \tag{11}$$

The compatibility conditions of the displacement, slope, moment and shear force at the junction of the two steps are as follows:

$$\left.\begin{aligned} &U_2 = U_3, && \mathrm{d}U_2/\mathrm{d}\beta = \mathrm{d}U_3/\mathrm{d}\beta \\ &EI_1 \frac{\mathrm{d}^2 U_2}{\mathrm{d}\beta^2} = EI_2 \frac{\mathrm{d}^2 U_3}{\mathrm{d}\beta^2}, && EI_1 \frac{\mathrm{d}^3 U_2}{\mathrm{d}\beta^3} = EI_2 \frac{\mathrm{d}^3 U_3}{\mathrm{d}\beta^3} \end{aligned}\right\} \beta = \beta_1, \tag{12}$$

$$\left.\begin{aligned} &U_3 = U_4, && \mathrm{d}U_3/\mathrm{d}\beta = \mathrm{d}U_4/\mathrm{d}\beta \\ &EI_2 \frac{\mathrm{d}^2 U_3}{\mathrm{d}\beta^2} = EI_3 \frac{\mathrm{d}^2 U_4}{\mathrm{d}\beta^2}, && EI_2 \frac{\mathrm{d}^3 U_3}{\mathrm{d}\beta^3} = EI_3 \frac{\mathrm{d}^3 U_4}{\mathrm{d}\beta^3} \end{aligned}\right\} \beta = \beta_2. \tag{13}$$

The continuity of displacement, moment and shear force at the crack location ($\beta = e/L$) can be written in the following form:

$$U_1 = U_2, \qquad \frac{\mathrm{d}^2 U_1}{\mathrm{d}\beta^2} = \frac{\mathrm{d}^2 U_2}{\mathrm{d}\beta^2}, \qquad \frac{\mathrm{d}^3 U_1}{\mathrm{d}\beta^3} = \frac{\mathrm{d}^3 U_2}{\mathrm{d}\beta^3}. \tag{14–16}$$

The crack is supposed to give rise to a jump in slope [10]. The transition can be written in the following form:

$$\frac{\mathrm{d}U_1}{\mathrm{d}x} + \frac{\mathrm{d}^2}{\mathrm{d}x^2}(EI_1 U_1)\frac{1}{K_t} = \frac{\mathrm{d}U_2}{\mathrm{d}x}.$$

Writing this in terms of β,

$$\frac{\mathrm{d}U_1}{\mathrm{d}\beta} + \frac{\lambda_1}{K}\frac{\mathrm{d}^2 U_1}{\mathrm{d}\beta^2} - \frac{\mathrm{d}U_2}{\mathrm{d}\beta} = 0, \tag{17}$$

where $K = K_t L/EI_1$ is the non-dimensional stiffness of the rotational spring representing the crack.

From the conditions (10)–(17), the characteristic equation for the problem is obtained:

$$\left|\begin{array}{cccccccccccccccc}
1 & 0 & 1 & 0 & 0 & 0 & 0 & 0 & 0 & 0 & 0 & 0 & 0 & 0 & 0 & 0 \\
0 & 1 & 0 & 1 & 0 & 0 & 0 & 0 & 0 & 0 & 0 & 0 & 0 & 0 & 0 & 0 \\
0 & 0 & 0 & 0 & 0 & 0 & 0 & 0 & 0 & 0 & 0 & 0 & \cosh\lambda_3 & \sinh\lambda_3 & -\cos\lambda_3 & -\sin\lambda_3 \\
0 & 0 & 0 & 0 & 0 & 0 & 0 & 0 & 0 & 0 & 0 & 0 & \sinh\lambda_3 & \cosh\lambda_3 & \sin\lambda_3 & -\cos\lambda_3 \\
0 & 0 & 0 & 0 & \cosh\alpha_1 & \sinh\alpha_1 & \cos\alpha_1 & \sin\alpha_1 & -\cosh\alpha_2 & -\sinh\alpha_2 & -\cos\alpha_2 & -\sin\alpha_2 & 0 & 0 & 0 & 0 \\
0 & 0 & 0 & 0 & \sinh\alpha_1 & \cosh\alpha_1 & -\sin\alpha_1 & \cos\alpha_1 & -F_1\sinh\alpha_1 & -F_1\cosh\alpha_2 & F_1\sin\alpha_2 & -F_1\cos\alpha_2 & 0 & 0 & 0 & 0 \\
0 & 0 & 0 & 0 & \cosh\alpha_1 & \sinh\alpha_1 & -\cos\alpha_1 & -\sin\alpha_1 & -G_1\cosh\alpha_2 & -G_1\sinh\alpha_2 & G_1\cos\alpha_2 & G_1\sin\alpha_2 & 0 & 0 & 0 & 0 \\
0 & 0 & 0 & 0 & \sinh\alpha_1 & \cosh\alpha_1 & \sin\alpha_1 & -\cos\alpha_1 & -H_1\sinh\alpha_2 & -H_1\cosh\alpha_2 & -H_1\sin\alpha_2 & H_1\cos\alpha_2 & 0 & 0 & 0 & 0 \\
0 & 0 & 0 & 0 & 0 & 0 & 0 & 0 & \cosh\alpha_3 & \sinh\alpha_3 & \cos\alpha_3 & \sin\alpha_3 & -\cosh\alpha_4 & -\sinh\alpha_4 & -\cos\alpha_4 & -\sin\alpha_4 \\
0 & 0 & 0 & 0 & 0 & 0 & 0 & 0 & \sinh\alpha_3 & \cosh\alpha_3 & -\sin\alpha_3 & \cos\alpha_3 & -F_2\sinh\alpha_4 & -F_2\cosh\alpha_4 & F_2\sin\alpha_4 & -F_2\cos\alpha_4 \\
0 & 0 & 0 & 0 & 0 & 0 & 0 & 0 & \cosh\alpha_3 & \sinh\alpha_3 & -\cos\alpha_3 & -\sin\alpha_3 & -G_2\cosh\alpha_4 & -G_2\sinh\alpha_4 & G_2\cos\alpha_4 & G_2\sin\alpha_4 \\
0 & 0 & 0 & 0 & 0 & 0 & 0 & 0 & \sinh\alpha_3 & \cosh\alpha_3 & \sin\alpha_3 & -\cos\alpha_3 & -H_2\sinh\alpha_4 & -H_2\cos\alpha_4 & -H_2\sin\alpha_4 & H_2\cos\alpha_4 \\
\cosh\alpha & \sinh\alpha & \cos\alpha & \sin\alpha & -\cosh\alpha & -\sinh\alpha & -\cos\alpha & -\sin\alpha & 0 & 0 & 0 & 0 & 0 & 0 & 0 & 0 \\
\cosh\alpha & \sinh\alpha & -\cos\alpha & -\sin\alpha & -\cosh\alpha & -\sinh\alpha & \cos\alpha & \sin\alpha & 0 & 0 & 0 & 0 & 0 & 0 & 0 & 0 \\
\sinh\alpha & \cosh\alpha & \sin\alpha & -\cos\alpha & -\sinh\alpha & -\cosh\alpha & -\sin\alpha & \cos\alpha & 0 & 0 & 0 & 0 & 0 & 0 & 0 & 0 \\
\frac{K}{\lambda_1}\sinh\alpha+\cosh\alpha & \frac{K}{\lambda_1}\cosh\alpha+\sinh\alpha & -\frac{K}{\lambda_1}\sin\alpha-\cos\alpha & \frac{K}{\lambda_1}\cos\alpha-\sin\alpha & -\frac{K}{\lambda_1}\sinh\alpha & -\frac{K}{\lambda_1}\cosh\alpha & \frac{K}{\lambda_1}\sin\alpha & -\frac{K}{\lambda_1}\cos\alpha & 0 & 0 & 0 & 0 & 0 & 0 & 0 & 0
\end{array}\right| = 0, \quad (18)$$

where $\alpha_1 = \lambda_1\beta_1$, $\alpha_2 = \lambda_2\beta_1$, $\alpha_3 = \lambda_2\beta_2$, $\alpha_4 = \lambda_3\beta_2$, $\alpha = \lambda_1 e/L$, $F_1 = \lambda_2/\lambda_1$, $G_1 = (\lambda_2/\lambda_1)^2(I_2/I_1)$, $H_1 = (\lambda_2/\lambda_1)^3(I_2/I_1)$, $F_2 = \lambda_3/\lambda_2$, $G_2 = (\lambda_3/\lambda_2)^2(I_3/I_2)$ and $H_2 = (\lambda_3/\lambda_2)^3(I_3/I_2)$. With every additional step, the characteristic equation will have four more rows and columns.

Equation (18) can be written in the short form

$$|\Delta| = 0.$$

Alternatively,

$$K = -\lambda_1 |\Delta_2| / |\Delta_1|, \tag{19}$$

where explicit forms of $|\Delta_1|$ and $|\Delta_2|$ are given by

$$|\Delta_1| = \left| \begin{array}{cccccccc}
1 & 0 & 1 & 0 & 0 & 0 & 0 & 0 \\
0 & 1 & 0 & 1 & 0 & 0 & 0 & 0 \\
0 & 0 & 0 & 0 & 0 & 0 & 0 & 0 \\
0 & 0 & 0 & 0 & 0 & 0 & 0 & 0 \\
0 & 0 & 0 & 0 & \cosh\alpha_1 & \sinh\alpha_1 & \cos\alpha_1 & \sin\alpha_1 \\
0 & 0 & 0 & 0 & \sinh\alpha_1 & \cosh\alpha_1 & -\sin\alpha_1 & \cos\alpha_1 \\
0 & 0 & 0 & 0 & \cosh\alpha_1 & \sinh\alpha_1 & -\cos\alpha_1 & -\sin\alpha_1 \\
0 & 0 & 0 & 0 & \sinh\alpha_1 & \cosh\alpha_1 & \sin\alpha_1 & -\cos\alpha_1 \\
0 & 0 & 0 & 0 & 0 & 0 & 0 & 0 \\
0 & 0 & 0 & 0 & 0 & 0 & 0 & 0 \\
0 & 0 & 0 & 0 & 0 & 0 & 0 & 0 \\
0 & 0 & 0 & 0 & 0 & 0 & 0 & 0 \\
\cosh\alpha & \sinh\alpha & \cos\alpha & \sin\alpha & -\cosh\alpha & -\sinh\alpha & -\cos\alpha & -\sin\alpha \\
\cosh\alpha & \sinh\alpha & -\cos\alpha & -\sin\alpha & -\cosh\alpha & -\sinh\alpha & \cos\alpha & \sin\alpha \\
\sinh\alpha & \cosh\alpha & \sin\alpha & -\cos\alpha & -\sinh\alpha & -\cosh\alpha & -\sin\alpha & \cos\alpha \\
\sinh\alpha & \cosh\alpha & -\sin\alpha & \cos\alpha & -\sinh\alpha & -\cosh\alpha & \sin\alpha & -\cos\alpha
\end{array} \right.$$

$$\left. \begin{array}{cccccccc}
0 & 0 & 0 & 0 & 0 & 0 & 0 & 0 \\
0 & 0 & 0 & 0 & 0 & 0 & 0 & 0 \\
0 & 0 & 0 & 0 & \cosh\lambda_3 & \sinh\lambda_3 & -\cos\lambda_3 & -\sin\lambda_3 \\
0 & 0 & 0 & 0 & \sinh\lambda_3 & \cosh\lambda_3 & \sin\lambda_3 & -\cos\lambda_3 \\
-\cosh\alpha_2 & -\sinh\alpha_2 & -\cos\alpha_2 & -\sin\alpha_2 & 0 & 0 & 0 & 0 \\
-F_1\sinh\alpha_2 & -F_1\cosh\alpha_2 & F_1\sin\alpha_2 & -F_1\cos\alpha_2 & 0 & 0 & 0 & 0 \\
-G_1\cosh\alpha_2 & -G_1\sinh\alpha_2 & G_1\cos\alpha_2 & G_1\sin\alpha_2 & 0 & 0 & 0 & 0 \\
-H_1\sinh\alpha_2 & -H_1\cosh\alpha_2 & -H_1\sin\alpha_2 & H_1\cos\alpha_2 & 0 & 0 & 0 & 0 \\
\cosh\alpha_3 & \sinh\alpha_3 & \cos\alpha_3 & \sin\alpha_3 & -\cosh\alpha_4 & -\sinh\alpha_4 & -\cos\alpha_4 & -\sin\alpha_4 \\
\sinh\alpha_3 & \cosh\alpha_3 & -\sin\alpha_3 & \cos\alpha_3 & -F_2\sinh\alpha_4 & -F_2\cosh\alpha_4 & F_2\sin\alpha_4 & -F_2\cos\alpha_4 \\
\cosh\alpha_3 & \sinh\alpha_3 & -\cos\alpha_3 & -\sin\alpha_3 & -G_2\cosh\alpha_4 & -G_2\sinh\alpha_4 & G_2\cos\alpha_4 & G_2\sin\alpha_4 \\
\sinh\alpha_3 & \cosh\alpha_3 & \sin\alpha_3 & -\cos\alpha_3 & -H_2\sinh\alpha_4 & -H_2\cosh\alpha_4 & -H_2\sin\alpha_4 & H_2\cos\alpha_4 \\
0 & 0 & 0 & 0 & 0 & 0 & 0 & 0 \\
0 & 0 & 0 & 0 & 0 & 0 & 0 & 0 \\
0 & 0 & 0 & 0 & 0 & 0 & 0 & 0 \\
0 & 0 & 0 & 0 & 0 & 0 & 0 & 0
\end{array} \right| \tag{20}$$

and

$$
|\Delta_2| = \left|\begin{array}{cccccccccccccccc}
1 & 0 & 1 & 0 & 0 & 0 & 0 & 0 & 0 & 0 & 0 & 0 & 0 & 0 & 0 & 0 \\
0 & 1 & 0 & 1 & 0 & 0 & 0 & 0 & 0 & 0 & 0 & 0 & 0 & 0 & 0 & 0 \\
0 & 0 & 0 & 0 & 0 & 0 & 0 & 0 & 0 & 0 & 0 & 0 & \cosh\lambda_3 & \sinh\lambda_3 & -\cos\lambda_3 & -\sin\lambda_3 \\
0 & 0 & 0 & 0 & 0 & 0 & 0 & 0 & 0 & 0 & 0 & 0 & \sinh\lambda_3 & \cosh\lambda_3 & \sin\lambda_3 & -\cos\lambda_3 \\
0 & 0 & 0 & 0 & \cosh\alpha_1 & \sinh\alpha_1 & \cos\alpha_1 & \sin\alpha_1 & -\cosh\alpha_2 & -\sinh\alpha_2 & -\cos\alpha_2 & -\sin\alpha_2 & 0 & 0 & 0 & 0 \\
0 & 0 & 0 & 0 & \sinh\alpha_1 & \cosh\alpha_1 & -\sin\alpha_1 & \cos\alpha_1 & -F_1\sinh\alpha_2 & -F_1\cosh\alpha_2 & F_1\sin\alpha_2 & -F_1\cos\alpha_2 & 0 & 0 & 0 & 0 \\
0 & 0 & 0 & 0 & \cosh\alpha_1 & \sinh\alpha_1 & -\cos\alpha_1 & -\sin\alpha_1 & -G_1\cosh\alpha_2 & -G_1\sinh\alpha_2 & G_1\cosh\alpha_2 & G_1\sinh\alpha_2 & 0 & 0 & 0 & 0 \\
0 & 0 & 0 & 0 & \sinh\alpha_1 & \cosh\alpha_1 & \sin\alpha_1 & -\cos\alpha_1 & -H_1\sinh\alpha_2 & -H_1\cosh\alpha_2 & -H_1\sin\alpha_2 & H_1\cos\alpha_2 & 0 & 0 & 0 & 0 \\
0 & 0 & 0 & 0 & 0 & 0 & 0 & 0 & \cosh\alpha_3 & \sinh\alpha_3 & \cos\alpha_3 & \sin\alpha_3 & -\cosh\alpha_4 & -\sinh\alpha_4 & -\cos\alpha_4 & -\sin\alpha_4 \\
0 & 0 & 0 & 0 & 0 & 0 & 0 & 0 & \sinh\alpha_3 & \cosh\alpha_3 & -\sin\alpha_3 & \cos\alpha_3 & -F_2\sinh\alpha_4 & -F_2\cosh\alpha_4 & F_2\sin\alpha_4 & -F_2\cos\alpha_4 \\
0 & 0 & 0 & 0 & 0 & 0 & 0 & 0 & \cosh\alpha_3 & \sinh\alpha_3 & -\cos\alpha_3 & -\sin\alpha_3 & -G_2\cosh\alpha_4 & -G_2\sinh\alpha_4 & G_2\cos\alpha_4 & G_2\sin\alpha_4 \\
0 & 0 & 0 & 0 & 0 & 0 & 0 & 0 & \sinh\alpha_3 & \cosh\alpha_3 & \sin\alpha_3 & -\cos\alpha_3 & -H_2\sinh\alpha_4 & -H_2\cosh\alpha_4 & -H_2\sin\alpha_4 & H_2\cos\alpha_4 \\
\cosh\alpha & \sinh\alpha & \cos\alpha & \sin\alpha & -\cosh\alpha & -\sinh\alpha & -\cos\alpha & -\sin\alpha & 0 & 0 & 0 & 0 & 0 & 0 & 0 & 0 \\
\cosh\alpha & \sinh\alpha & -\cos\alpha & -\sin\alpha & -\cosh\alpha & -\sinh\alpha & \cos\alpha & \sin\alpha & 0 & 0 & 0 & 0 & 0 & 0 & 0 & 0 \\
\sinh\alpha & \cosh\alpha & \sin\alpha & -\cos\alpha & -\sinh\alpha & -\cosh\alpha & -\sin\alpha & \cos\alpha & 0 & 0 & 0 & 0 & 0 & 0 & 0 & 0 \\
\cosh\alpha & \sinh\alpha & -\cos\alpha & -\sin\alpha & 0 & 0 & 0 & 0 & 0 & 0 & 0 & 0 & 0 & 0 & 0 & 0
\end{array}\right| \tag{21}
$$

2.1. METHODOLOGY FOR CRACK DETECTION For the beam, the first three natural frequencies are measured. Using one of the frequencies and assuming a particular value for e, the non-dimensionalized stiffness K is computed from equation (19). Thereby a variation of stiffness with crack location is obtained. Similar curves can be plotted for another two natural frequencies. Since physically there is only one crack, the position at which the three curves intersect gives the crack location [11]. The crack size is then obtained using the relationship between stiffness K and crack size a.

3. CASE STUDY

The formulation for a beam with three steps is indicated. To verify the method, a beam with two steps (see Figure 2(a)) is taken up for a case study. The explicit forms of $|\Delta_1|$

and $|\Delta_2|$ for this case are given below:

$$|\Delta_1| = \begin{vmatrix} 1 & 0 & 1 & 0 & 0 & 0 & 0 & 0 & 0 & 0 & 0 & 0 \\ 0 & 1 & 0 & 1 & 0 & 0 & 0 & 0 & 0 & 0 & 0 & 0 \\ 0 & 0 & 0 & 0 & 0 & 0 & 0 & 0 & \cosh\lambda_2 & \sinh\lambda_2 & -\cos\lambda_2 & -\sin\lambda_2 \\ 0 & 0 & 0 & 0 & 0 & 0 & 0 & 0 & \sinh\lambda_2 & \cosh\lambda_2 & \sin\lambda_2 & -\cos\lambda_2 \\ 0 & 0 & 0 & 0 & \cosh\alpha_1 & \sinh\alpha_1 & \cos\alpha_1 & \sin\alpha_1 & -\cosh\alpha_2 & -\sinh\alpha_2 & -\cos\alpha_2 & -\sin\alpha_2 \\ 0 & 0 & 0 & 0 & \sinh\alpha_1 & \cosh\alpha_1 & -\sin\alpha_1 & \cos\alpha_1 & -F_1\sinh\alpha_2 & -F_1\cosh\alpha_2 & F_1\sin\alpha_2 & -F_1\cos\alpha_2 \\ 0 & 0 & 0 & 0 & \cosh\alpha_1 & \sinh\alpha_1 & -\cos\alpha_1 & -\sin\alpha_1 & -G_1\cosh\alpha_2 & -G_1\sinh\alpha_2 & G_1\cos\alpha_2 & G_1\sin\alpha_2 \\ 0 & 0 & 0 & 0 & \sinh\alpha_1 & \cosh\alpha_1 & \sin\alpha_1 & -\cos\alpha_1 & -H_1\sinh\alpha_2 & -H_1\cosh\alpha_2 & -H_1\sin\alpha_2 & H_1\cos\alpha_2 \\ \cosh\alpha & \sinh\alpha & \cos\alpha & \sin\alpha & -\cosh\alpha & -\sinh\alpha & -\cos\alpha & -\sin\alpha & 0 & 0 & 0 & 0 \\ \cosh\alpha & \sinh\alpha & -\cos\alpha & -\sin\alpha & -\cosh\alpha & -\sinh\alpha & \cos\alpha & \sin\alpha & 0 & 0 & 0 & 0 \\ \sinh\alpha & \cosh\alpha & \sin\alpha & -\cos\alpha & -\sinh\alpha & -\cosh\alpha & -\sin\alpha & \cos\alpha & 0 & 0 & 0 & 0 \\ \sinh\alpha & \cosh\alpha & -\sin\alpha & \cos\alpha & -\sinh\alpha & -\cosh\alpha & \sin\alpha & -\cos\alpha & 0 & 0 & 0 & 0 \end{vmatrix}, \quad (22)$$

$$|\Delta_2| = \begin{vmatrix} 1 & 0 & 1 & 0 & 0 & 0 & 0 & 0 & 0 & 0 & 0 & 0 \\ 0 & 1 & 0 & 1 & 0 & 0 & 0 & 0 & 0 & 0 & 0 & 0 \\ 0 & 0 & 0 & 0 & 0 & 0 & 0 & 0 & \cosh\lambda_2 & \sinh\lambda_2 & -\cos\lambda_2 & -\sin\lambda_2 \\ 0 & 0 & 0 & 0 & 0 & 0 & 0 & 0 & \sinh\lambda_2 & \cosh\lambda_2 & \sin\lambda_2 & -\cos\lambda_2 \\ 0 & 0 & 0 & 0 & \cosh\alpha_1 & \sinh\alpha_1 & \cos\alpha_1 & \sin\alpha_1 & -\cosh\alpha_2 & -\sinh\alpha_2 & -\cos\alpha_2 & -\sin\alpha_2 \\ 0 & 0 & 0 & 0 & \sinh\alpha_1 & \cosh\alpha_1 & -\sin\alpha_1 & \cos\alpha_1 & -F_1\sinh\alpha_2 & -F_1\cosh\alpha_2 & F_1\sin\alpha_2 & -F_1\cos\alpha_2 \\ 0 & 0 & 0 & 0 & \cosh\alpha_1 & \sinh\alpha_1 & -\cos\alpha_1 & -\sin\alpha_1 & -G_1\cosh\alpha_2 & -G_1\sinh\alpha_2 & G_1\cos\alpha_2 & G_1\sin\alpha_2 \\ 0 & 0 & 0 & 0 & \sinh\alpha_1 & \cosh\alpha_1 & \sin\alpha_1 & -\cos\alpha_1 & -H_1\sinh\alpha_2 & -H_1\cosh\alpha_2 & -H_1\sin\alpha_2 & H_1\cos\alpha_2 \\ \cosh\alpha & \sinh\alpha & \cos\alpha & \sin\alpha & -\cosh\alpha & -\sinh\alpha & -\cos\alpha & -\sin\alpha & 0 & 0 & 0 & 0 \\ \cosh\alpha & \sinh\alpha & -\cos\alpha & -\sin\alpha & -\cosh\alpha & -\sinh\alpha & \cos\alpha & \sin\alpha & 0 & 0 & 0 & 0 \\ \sinh\alpha & \cosh\alpha & \sin\alpha & -\cos\alpha & -\sinh\alpha & -\cosh\alpha & -\sin\alpha & \cos\alpha & 0 & 0 & 0 & 0 \\ \cosh\alpha & \sinh\alpha & -\cos\alpha & -\sin\alpha & 0 & 0 & 0 & 0 & 0 & 0 & 0 & 0 \end{vmatrix}. \quad (23)$$

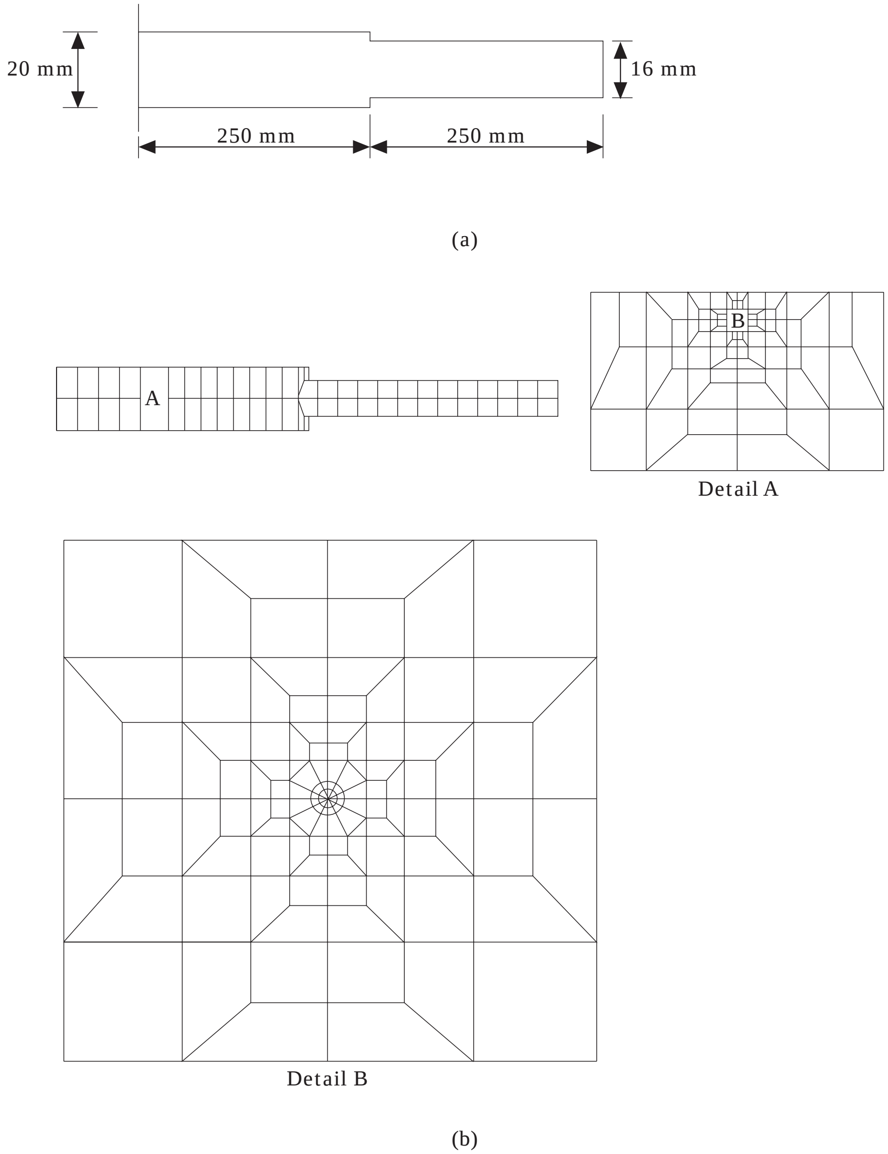

Figure 2. (a) The beam for the case study: thickness = 12 mm. (b) The finite element discretization for case 2: $e = 100$ mm, $a/h = 0{\cdot}1$, elements = 260, nodes = 863.

The material data are as follows: modulus of elasticity, $E = 2{\cdot}1 \times 10^{11}$ N/m^2; density, $\rho = 7860$ kg/m^3; Poisson's ratio $\nu = 0{\cdot}3$. Eight crack locations are considered for prediction. The natural frequencies for both the uncracked and cracked geometries are computed by the finite element method. For this purpose, the beam is discretized by eight-noded isoparametric elements (see Figure 2(b)). Around the crack tip, 12 quarter-point singularity elements are used. The natural frequencies thus obtained are shown in Table 1.

While applying the method to the present problem, it is found that the three curves do not intersect at a common point in a number of cases; e.g., case 1 (see Figure 3). In order to avoid this difficulty, a scheme, which is a sort of calibration of modulus of elasticity, suggested in reference [13], is employed. The modulus of elasticity used as an input in the

TABLE 1

The crack location and size considered for the case study and the finite element based natural frequencies.

Case number	Crack position, β	Crack size, a/h	Natural frequencies (rad/s) ω_1	ω_2	ω_3
	Uncracked	Uncracked	455·0	2345·9	6506·7
1	0·05	0·10	451·5	2334·0	6483·7
2	0·20	0·10	453·0	2345·7	6498·4
3	0·40	0·10	454·2	2341·6	6488·3
4	0·45	0·10	454·4	2340·1	6499·4
5	0·20	0·20	447·6	2344·6	6480·9
6	0·20	0·30	438·3	2342·7	6448·3
7	0·20	0·40	423·8	2339·7	6398·3
8	0·20	0·50	402·2	2335·5	6323·1

analytical approach (equation (19)) for each mode is calculated using the FEM based uncracked natural frequency for the corresponding mode.

With this sort of "zero setting" the curves are plotted for all of the eight cases (see Figure 4). Figure 3 may be misread to give rise to a crack location at $\beta = 0{\cdot}45$ as against the actual $\beta = 0{\cdot}05$. There is a tremendous improvement in the prediction only after the zero setting (case 1, Figure 4). For all of the cases, the three plots for three natural frequencies intersect and give the location of the crack. In some cases, the intersection point cannot be easily read from the graph because of the scale. With magnification (see Figure 5) this difficulty is eliminated.

To eliminate the subjective error involved in the graphical procedure, an alternative numerical method is possible. The intersection point (K_1, β_1) for the pair of curves corresponding to ω_1 and ω_2 is obtained. The similar intersections (K_2, β_2) and (K_3, β_3) are obtained for the other two pairs (ω_1 and ω_3; ω_2 and ω_3). The averages of the three intersection points, that is, $K = \frac{1}{3}\Sigma K_i$ and $\frac{1}{3}\Sigma \beta_i$, are taken as the prediction. The intersection points (K_1, β_1), (K_2, β_2) and (K_3, β_3) must be selected judiciously. The crack size is obtained using the formulae given in reference [12]. The relationship between K and

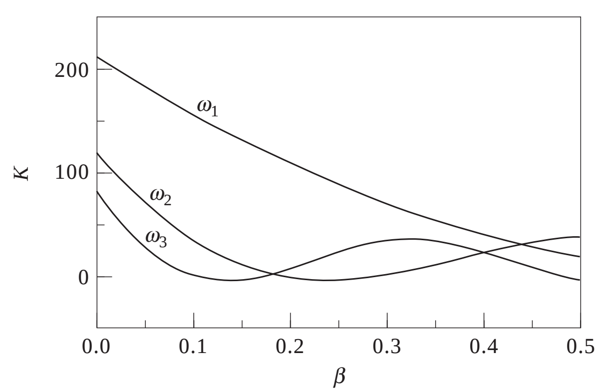

Figure 3. The variation of stiffness with location for case 1, for three fundamental modes, without any common point of intersection (without zero setting).

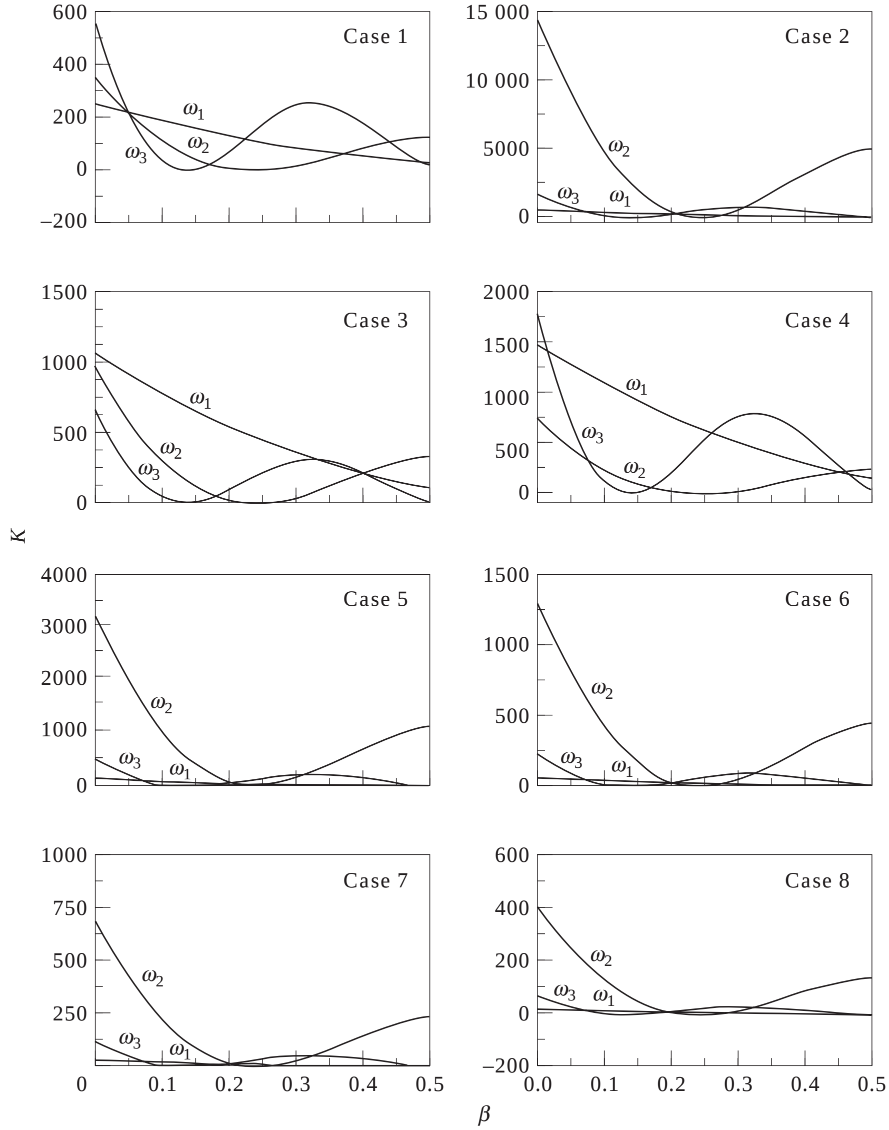

Figure 4. The variation of stiffness with location for three fundamental modes.

crack size (a/h) is as follows:

$$K = \frac{bh^2L}{72\pi I(a/h)^2 f(a/h)}, \tag{24}$$

where

$$f(a/h) = 0{\cdot}6384 - 1{\cdot}035(a/h) + 3{\cdot}7201(a/h)^2 - 5{\cdot}1773(a/h)^3 + 7{\cdot}553(a/h)^4 - 7{\cdot}332(a/h)^5 + 2{\cdot}4909(a/h)^6 \tag{25}$$

and b and h are the thickness and height, respectively, of the beam.

A comparison of the computed crack location and size with the actual values is given in Table 2. The accuracy of prediction is good.

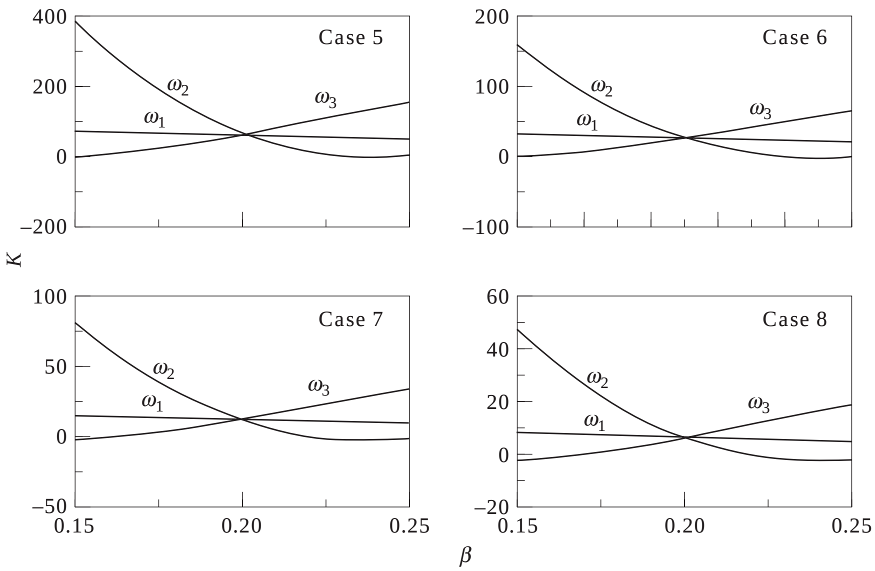

Figure 5. The variation of stiffness with location, replotted at a larger scale, for four cases shown in Figure 4.

TABLE 2

A comparison of the predicted and actual crack location and size

	Actual crack		Predicted crack				
Case number	Location, β	Size, a/h	Location, β	% error	Stiffness, K	Size, a/h	% error
1	0·05	0·10	0·0494	−1·20	215·77	0·1042	4·22
2	0·20	0·10	0·2061	3·05	224·96	0·1020	1·99
3	0·40	0·10	0·4028	0·70	220·36	0·1031	3·09
4	0·45	0·10	0·4583	1·84	229·78	0·1009	0·87
5	0·20	0·20	0·2013	0·65	62·48	0·1967	−1·65
6	0·20	0·30	0·2004	0·20	25·95	0·2999	−0·02
7	0·20	0·40	0·2001	0·05	13·02	0·4053	1·33
8	0·20	0·50	0·2002	0·10	6·96	0·5212	4·24

4. CONCLUSIONS

A method for detection of the location and size of a crack in a stepped cantilever beam has been presented. The details of the method are given. The accuracy of the method is illustrated by a case study involving a two-step beam. The method predicts the location of crack quite accurately. The error in prediction of the location is always less than about 3%. The crack size is also predicted accurately; the error is again less than 4·5%. The procedure can easily be adapted for more steps and for a crack located in any of the segments.

REFERENCES

1. R. D. Adams, D. Walton, J. E. Flitcroft and D. Short 1975 *Composite Reliability*, *ASTM STP* 580, 159–175. Philadelphia: American Society for Testing Materials. Vibration testing as a nondestructive test tool for composite materials.

2. H. J. Petroski 1981 *International Journal of Fracture* **17**, R71–R76. Simple static and dynamic models for the cracked elastic beam.
3. B. Grabowski 1979 *Journal of Mechanical Design* **102**, 140–146. The vibrational behaviour of a turbine rotor containing a transverse crack.
4. I. W. Mayes and W. G. R. Davies 1976 *Institution of Mechanical Engineers Conference Publication "Vibrations in Rotating Machinery", Paper C* 168/76. The vibrational behaviour of a rotating shaft system containing a transverse crack.
5. S. Christides and A. D. S. Barr 1984 *International Journal of Mechanical Sciences* **26**, 639–648. One-dimensional theory of cracked Bernoulli–Euler beams.
6. A. D. Dimarogonas and S. A. Paipetis 1983 *Analytical Methods in Rotor Dynamics*. London: Applied Science Publishers.
7. A. D. Dimarogonas and C. A. Papadopoulos 1983 *Journal of Sound and Vibration* **91**, 583–593. Vibration of cracked shafts in bending.
8. C. A. Papadopoulos and A. D. Dimarogonas 1983 *Transactions of the American Society of Mechanical Engineers*, *Journal of Vibration*, *Acoustics*, *Stress*, *and Reliability in Design* **110**(1), 1–8. Coupled longitudinal and bending vibrations of a cracked shaft.
9. T. G. Chondros and A. D. Dimarogonas 1980 *Journal of Sound and Vibration* **69**, 531–538. Identification of cracks in welded joints of complex structures.
10. P. F. Rizos, N. Aspragathos and A. D. Dimarogonas 1990 *Journal of Sound and Vibration* **138**, 381–388. Identification of crack location and magnitude in a cantilever beam from the vibration modes.
11. R. Y. Liang, F. K. Choy and J. Hu 1991 *Journal of the Franklin Institute* **328**(4), 505–518. Detection of cracks in beam structures using measurements of natural frequencies.
12. W. M. Ostachowicz and M. Krawkczuk 1991 *Journal of Sound and Vibration* **150**, 191–201. Analysis of the effect of cracks on the natural frequencies of a cantilever beam.
13. R. D. Adams, P. Cawley, C. J. Pye and B. J. Stone 1978 *Journal of Mechanical Engineering Science* **20**(2), 93–100. A vibration technique for non-destructively assessing the integrity of structures.
14. P. Cawley and R. D. Adams 1979 *Journal of Strain Analysis* **14**(2), 49–57. The location of defects in structure from measurements of natural frequencies.
15. T. Y. Kam and T. Y. Lee 1991 *Engineering Fracture Mechanics* **42**(2), 381–387. Detection of cracks in structures using modal test data.
16. A. K. Pandey, M. Biswas and M. M. Samman 1991 *Journal of Sound and Vibration* **145**, 321–332. Damage detection from changes in curvature mode shapes.
17. A. K. Pandey and M. Biswas 1994 *Journal of Sound and Vibration* **169**, 3–17. Damage detection in structures using changes in flexibility.